ESR of Gd^{3+} and Er^{3+} in $Pr_{2-x}Ce_xCuO_4$

G.B. Martins, D. Rao, J.A. Valdivia, M.A. Pires, G.E. Barberis, and C. Rettori
Instituto de Física "Gleb Wataghin," Universidade Estadual de Campinas, 13083-970, Campinas, São Paulo, Brazil

P. A. Venegas
Departamento de Física, Universidade Estadual Paulista, 17033-360, Bauru, São Paulo, Brazil

S. Oseroff
San Diego State University, San Diego, California 92182

Z. Fisk
Los Alamos National Laboratory, Los Alamos, New Mexico 87545
(Received 14 October 1994)

Electron spin resonance (ESR) of Gd^{3+} and Er^{3+} in single crystals of $Pr_{2-x}Ce_xCuO_4$ ($0 \leq x \leq 0.15$) at liquid-helium temperature shows crystal-field (CF) effects corresponding to a C_{4v} point symmetry. Upon doping with Ce^{4+}, a reduction of about 23% in the second-order CF parameter $|b_{20}|$ is found with no significant change for the other CF spin-Hamiltonian parameters. The resonance lines broaden and present a Dysonian line shape at higher Ce^{4+} concentration, which is consistent with an increase in the CF inhomogeneity and the metallic character of the compound. Magnetic-susceptibility measurements present a small increase in the low-temperature anisotropy upon doping, consistent with a smaller $\langle |B_0^2| \rangle$ crystal-field parameter for Pr^{3+} in $Pr_{2-x}Ce_xCuO_4$. The reduction in the CF parameters is tentatively attributed to charge transfer from Ce atoms to the CuO_2 planes. The exchange parameters $j_{Gd\text{-}Pr}$ and $j_{Pr\text{-}Pr}$ are estimated from the ESR and susceptibility measurements.

I. INTRODUCTION

Among the R_2CuO_4 (2:1:4) compounds, where R=rare-earth, those with R = Pr, Nd, and Sm have attracted increased attention since the discovery that superconductivity can be induced in them by substituting Ce for the R.[1,2] This family of superconductors is quite different from the one based on R=La. The La compounds are orthorhombic and superconductivity is achieved by oxidation of the CuO_2 planes (hole doping). This is usually achieved by replacing Sr^{2+} or Ba^{2+} for La^{3+} ions or by oxidizing the sample at high temperature and high oxygen pressure,[3] or even electrochemically.[4,5] On the other hand, for R=Pr, Nd, and Sm the compounds are tetragonal and the substitution of Ce^{4+} for R^{3+} ions reduces the CuO_2 planes (electron doping). It is now known that after thermal treatment in a reducing atmosphere, these cuprates become n-type superconductors (negative carriers).[2] Because of their simpler crystal structure, with planar CuO_2 layers and no apical oxygens, the study of these n-type superconductors may lead to a better understanding of the fundamental mechanisms of superconductivity in these high-temperature superconductors (HTS).

A common feature of all the 2:1:4 cuprates is that they must be doped in order to achieve superconductivity. It is expected that charge transfer associated with the doping process may locally affect the crystalline electric field (CEF). Various experimental techniques have been used to probe the local CEF: inelastic neutron scattering (INS),[6] magnetic susceptibility,[7] CF excitations in Raman scattering,[8] electron spin resonance (ESR),[9] nuclear quadrupole resonance (NQR),[10] etc.

Here we present the results of a systematic ESR study at X band of $\sim 0.5\%$ of Gd^{3+} and Er^{3+}, in single crystals of $Pr_{2-x}Ce_xCuO_4$($0 \leq x \leq 0.15$). We also report the results from magnetic susceptibility and ESR experiments on natural impurities of Gd^{3+} in single crystals of Pr_2CuO_4 and $Pr_{1.85}Ce_{.15}CuO_4$.

II. EXPERIMENT

The samples were grown from nominal stoichiometric mixtures of the corresponding oxides, using PbO- and CuO-based fluxes in platinum crucibles.[11] Typical crystal sizes were $3 \times 4 \times 0.3$ mm^3, with the c-axis oriented along the smaller dimension. Our samples were not subjected to reducing thermal treatment, i.e., all our results are for the normal state. The ESR experiments were carried out using a Varian E-line spectrometer with a liquid-helium tail Dewar adapted to a room temperature rectangular TE_{102} cavity. The susceptibility measurements were made with a Quantum Design dc SQUID magnetometer.

III. RESULTS AND ANALYSIS

Figure 1 shows the observed ESR spectra of $\sim 0.5\%$ of Gd^{3+} for several $Pr_{2-x}Ce_xCuO_4$ crystals at liquid-

helium temperature, with the magnetic field parallel to the c axis. Figure 2 shows the anisotropy of the spectra for three samples of Fig. 1, when the magnetic field is rotated in the (010) plane. Figure 3 shows the anisotropy of the spectra for the undoped ($x = 0$) and doped ($x = 0.15$) crystals when the magnetic field is rotated perpendicular to the c axis. In every case the anisotropy is well described by the spin Hamiltonian appropriate to C_{4v} point symmetry:[12]

$$\hat{H} = g_{\|}\mu_B H_z S_z + g_{\perp}\mu_B (H_x S_x + H_y S_y) + b_{20}O_{20} + b_{40}O_{40} + b_{44}O_{44}, \quad (1)$$

where $g_{\|}$ and $g_{\perp}$ are the gyromagnetic factors for the magnetic field parallel and perpendicular to the c axis, respectively. Here μ_B is the Bohr magneton, O_{nm} are Stevens' operators, and b_{nm} are the corresponding CF parameters. In Eq. (1) we considered spin operators up

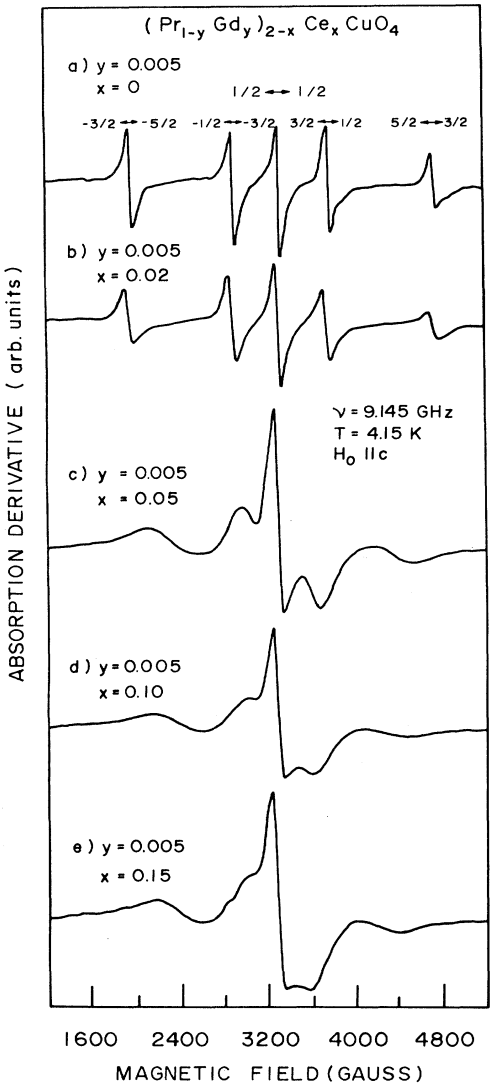

FIG. 1. ESR spectra of Gd^{3+} in $Pr_{2-x}Ce_xCuO_4$ for $0 \leq x \leq 0.15$ and $\vec{H}_0 \parallel c$.

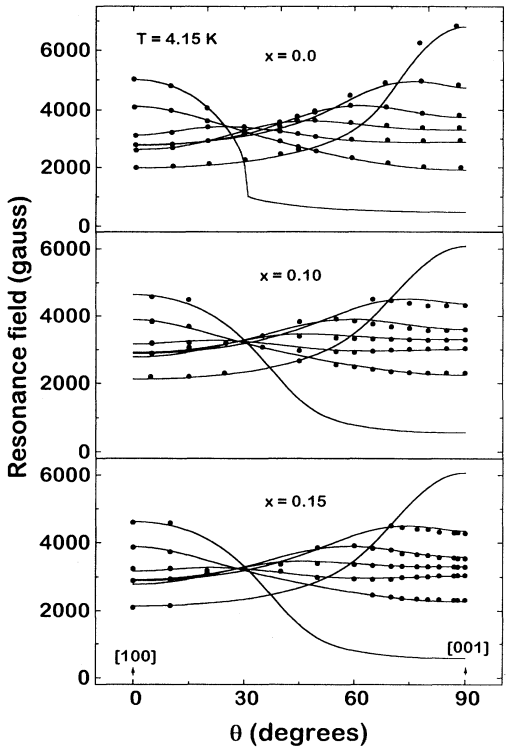

FIG. 2. Angular dependence of the ESR spectra in the (010) plane for Gd^{3+} in $Pr_{2-x}Ce_xCuO_4$ ($x = 0$, 0.1, 0.15). The solid lines are the best fit to Eq. (1) (see text).

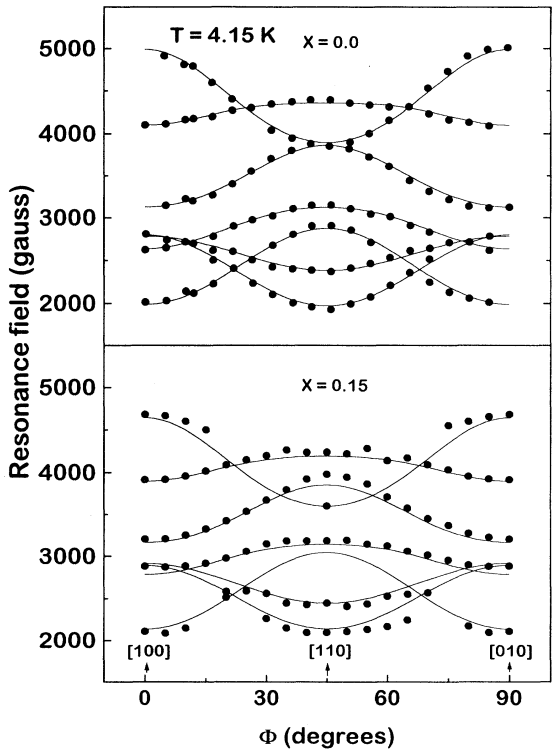

FIG. 3. Angular dependence of the ESR spectra in the (001) plane for Gd^{3+} in $Pr_{2-x}Ce_xCuO_4$ ($x = 0$, 0.15). The solid lines are the best fit to Eq. (1) (see text).

to fourth order only, because the values of the sixth order CF parameters are in the range of our experimental error. The solid lines in Figs. 2 and 3 are the best fits of the data to Eq. (1). Since the Zeeman effect is of the same order of magnitude as the crystal-field splitting, the fitting parameters were obtained by complete diagonalization of the spin Hamiltonian in Eq. (1) and a self-consistent calculation of the magnetic field for every transition. Table I shows the fitting parameters obtained at liquid-helium temperature. Since the Zeeman effect is independent of Ce concentration, the g values are not included in Table I. The values obtained at 4.15 K were $g_{\|} = 1.985 \pm 0.005$, and $g_{\perp} = 2.040 \pm 0.005$. The anisotropy $(g_{\perp} - g_{\|})$ was found to be smaller (~ 0.02) at liquid-nitrogen temperature (see below).

Figure 4 shows the simulated spectra corresponding to Fig 1. These spectra were calculated using the parameters given in Table I, the appropriate transition probabilities, and the Boltzmann population factors for each transition. Dysonian line shapes[13] with increasing metallic character at higher Ce^{4+} concentration were also used in Fig. 4. We considered linewidths proportional to the matrix elements of the O_{20} operator for each transition, with increasing values for higher Ce^{4+} concentrations. The broadening may be attributed to the CF inhomogeneities produced by the doping.

Our data indicate that in addition to a consistently increasing inhomogeneity and metallic character of the samples, associated with the Ce^{4+} doping process, there is a reduction of about 23% in the second-order CF parameter $|b_{20}|$ at the Gd^{3+} site (see Table I). From a simple point charge model,[14] and in view of the reduction in the lattice parameters due to the substitution of Ce^{4+} for Pr^{3+} ions,[15] one would expect an increase in $|b_{20}|$. Instead, our ESR results suggest that the observed reduction in the CF parameter $|b_{20}|$ may be attributed to charge transfer effects.

In order to see to what extent the change in the second order CF parameter $|b_{20}|$ of an S-state ion (Gd^{3+},$4f^7$) can also be observed in a non-S-state ion (Pr^{3+},$4f^2$),[16] we measured the magnetic susceptibility of two single crystals, Pr_2CuO_4 and $Pr_{1.85}Ce_{.15}CuO_4$. Figure 5 shows the magnetic susceptibility parallel ($\chi_{\|}$) and perpendicular ($\chi_{\perp}$) to the c axis for both crystals. The solid lines in Fig. 5 are the theoretically calculated ($\chi_{\|,\perp}$) magnetic susceptibility:[17]

$$\chi_{\|,\perp} = \frac{\chi^{\mathrm{CF}}_{\|,\perp}}{1 - j_{\mathrm{Pr-Pr}}(\frac{g_J - 1}{g_J})^2 \frac{\chi^{\mathrm{CF}}_{\|,\perp}}{\mu_B^2 N_0}} + cN_0 \frac{(g\mu_B)^2 S(S+1)}{3k_B T}, \quad (2)$$

TABLE I. Crystal-field parameters for Gd^{3+} in $Pr_{2-x}Ce_xCuO_4$, b_{nm} (10^{-4} cm^{-1}), at 4.15 K.

x	b_{20}	b_{40}	b_{44}[a]
0	-417(5)	-36(2)	42(2)
0.02	-411(5)	-35(2)	40(2)
0.05	-350(10)	-32(3)	40(3)
0.10	-324(20)	-31(4)	40(4)
0.15	-320(20)	-32(4)	40(4)

[a]See Ref. 25.

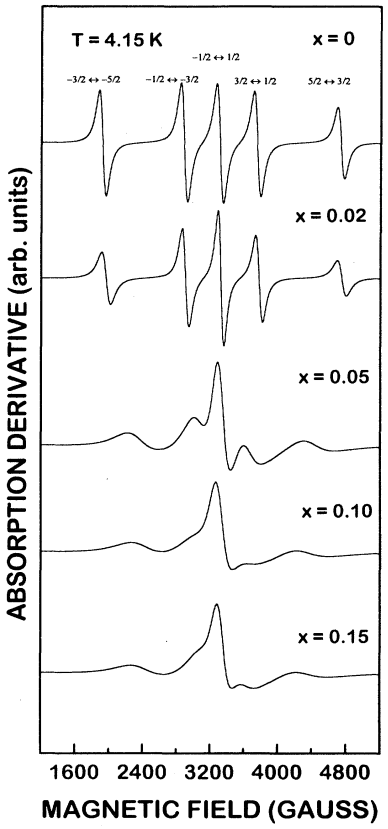

FIG. 4. Simulated ESR spectra (see text) for Gd^{3+} in $Pr_{2-x}Ce_xCuO_4$ corresponding to the spectra in Fig. 1.

where $\chi^{\mathrm{CF}}_{\|,\perp}$ is the Pr^{3+} CF-only magnetic susceptibility, $j_{\mathrm{Pr-Pr}}$ is the total Pr^{3+}-Pr^{3+} exchange interaction, g_J the Pr^{3+} Landé g factor, N_0 Avogadro's number, and c the concentration of natural impurities relative to Pr, which are assumed to be mainly Gd^{3+} ($g = 2$, $S = 7/2$). In the calculation of $\chi^{\mathrm{CF}}_{\|,\perp}$, all the excited states of Pr^{3+} were taken into account. We used the intermediate coupling approach[18] and the CF parameters obtained from Raman experiments.[19] The host Pr^{3+}-Pr^{3+} exchange interaction was introduced in Eq. (2) as a molecular field (MF) term. Since we have not seen any splitting of the ESR lines due to antiferromagnetic ordering of the copper ions,[20,21] we have not taken into consideration any contribution from the copper spins in Eq. (2). For the Ce doped sample, a weighted susceptibility $\chi_{\|,\perp} = \sum_i n_i \chi^i_{\|,\perp}$ was used in order to account for the various Pr^{3+} sites observed in Raman and INS experiments.[6,19] The weighting factors n_i were obtained from the relative Raman line intensities corresponding to the two sets of sites (sites I, II, IIIa, and sites I, II, IIIb).[19] The calculated magnetic susceptibility was found to give basically the same result for both sets of sites. Table II displays the set of parameters used in the calculation of $\chi_{\|,\perp}$ for Pr_2CuO_4 and $Pr_{1.85}Ce_{.15}CuO_4$. The exchange parameter $j_{\mathrm{Pr-Pr}}$, within the accuracy of the experiment, did not depend on the Ce^{4+} doping. This is consistent with a very small decrease in the R ordering temperature

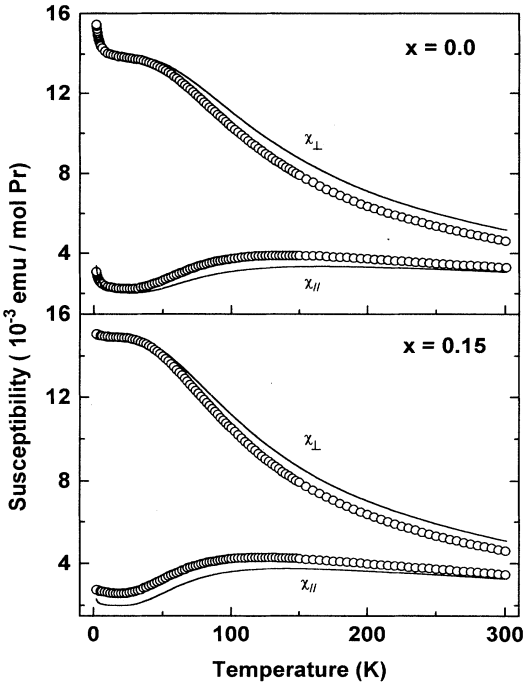

FIG. 5. Temperature dependence of the magnetic susceptibility (χ) for $Pr_{2-x}Ce_xCuO_4$ (x = 0, 0.15). $\chi_\parallel$ and $\chi_\perp$ correspond to the magnetic field paralell and perpendicular to the c axis. The applied magnetic field was 10 kOe. The solid lines are the calculated susceptibilities using Eq. (2) (see text).

found for the Nd-based (Ref. 22) and Sm-based (Ref. 23) compounds diluted with Ce^{4+}. The temperature dependence of the magnetic susceptibility $\chi_{\parallel,\perp}$, calculated using the parameters of Table II and presented in Fig. 5, differs from the high-temperature data. We believe that the difference can be attributed to a temperature dependence of the CF parameters. Some indication for such dependence is suggested by the Raman shift of the 156 cm^{-1} CF excitation at high temperatures.[8]

The existence of an exchange interaction between the R's would certainly introduce a g shift in the Gd^{3+} resonance. The g shift in the MF approximation can be written[17]

$$\Delta g_{\parallel,\perp} = [(g_J - 1)/g_J] \left(\frac{\chi_{\parallel,\perp}}{\mu_B^2 N_0} \right) j_{\text{Gd-Pr}}, \qquad (3)$$

where $j_{\text{Gd-Pr}}$ is the total exchange interaction ($j_{\text{Gd-Pr}} = \sum_k j^k_{\text{Gd-Pr}}$) between the Gd^{3+} and the surrounding Pr^{3+} ions. Equation (3) predicts a smaller g-value anisotropy ($g_\parallel - g_\perp$) at higher temperatures, in agreement with our observations (see above). Using Eq. (3) and the low-temperature g values, we estimated, within the accuracy of the measurement, $j_{\text{Gd-Pr}} \cong -0.5$ meV in Pr_2CuO_4 and $Pr_{1.85}Ce_{.15}CuO_4$. This value is 1 order of magnitude smaller than $j_{\text{Pr-Pr}}$ (see Table II), suggesting a trend toward stronger exchange interaction between R's with larger ionic radius.

Figure 6 shows the ESR spectra of natural impurities of Gd^{3+} for the same two crystals used in the susceptibility experiment. The presence of natural Gd^{3+} impurities in the crystals is also evidenced by the small increase in susceptibility at low-temperature shown in Fig. 5. The ESR spectra for these natural impurities are consistent with those for Gd^{3+}-doped crystals given above. We also studied the effect of Ce^{4+} doping on the ESR spectra of the non-S-state Er^{3+}. Figure 7 shows the ESR spectra of Er^{3+} in $Pr_{2-x}Ce_xCuO_4$ for the magnetic field parallel

TABLE II. Pr^{3+} crystal-field parameters B^k_q (meV), exchange parameters $j_{R\text{-}R}$ (meV), Gd^{3+} concentration c (ppm, relative to Pr) and weighting factors n_i used in the calculated magnetic susceptibility.

	Pr_2CuO_4		$Pr_{1.85}Ce_{.15}CuO_4$			
B^k_q	INS[a]	Raman[b]	Site I	Site II	Site IIIa	Site IIIb
B^2_0	-28	-30	-30	-17	-35	-29
B^2_2	0	0	0	0	0	4
B^4_0	-301	-275	-285	-297	-250	-275
B^6_0	26	21	25	41	19	21
B^4_4	228	228	228	228	228	228
B^6_4	224	224	224	224	224	224
$j_{\text{Pr-Pr}}$	-7(1)			-7(1)		
$j_{\text{Gd-Pr}}$	-0.5(1)			-0.5(2)		
c	~ 350			~ 70		
n_i[c]			0.31	0.45	-	0.24
n_i[d]			0.46	0.42	0.12	-

[a]From Ref. 6.
[b]From Ref. 19.
[c]Case 1 from Ref. 19.
[d]Case 2 from Ref. 19.

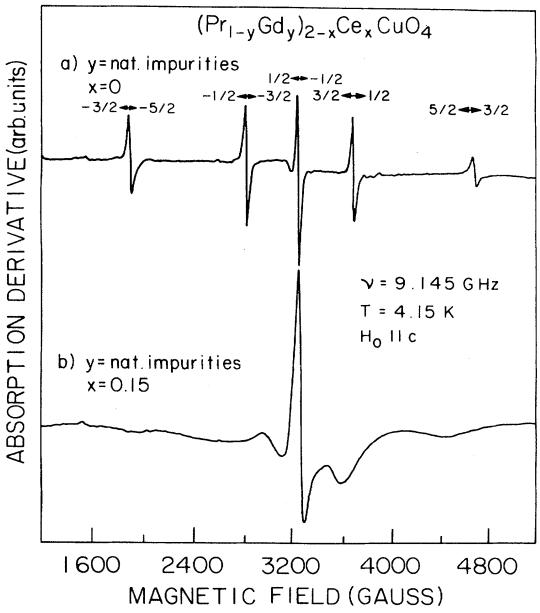

FIG. 6. ESR spectra of Gd^{3+} natural impurities in $Pr_{2-x}Ce_xCuO_4$ (x= 0, 0.15) for $\vec{H}_0 \parallel c$. These spectra were obtained from the same samples used in the susceptibility experiments of Fig. 5.

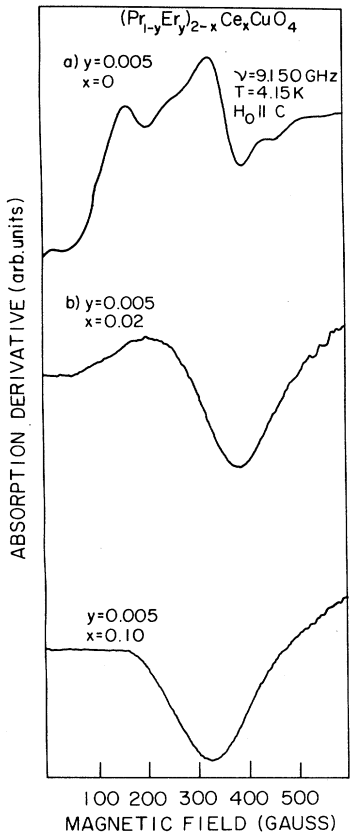

FIG. 7. ESR spectra of Er^{3+} in $Pr_{2-x}Ce_xCuO_4$ ($x = 0$, 0.02, 0.05) for $\vec{H}_0 \parallel c$.

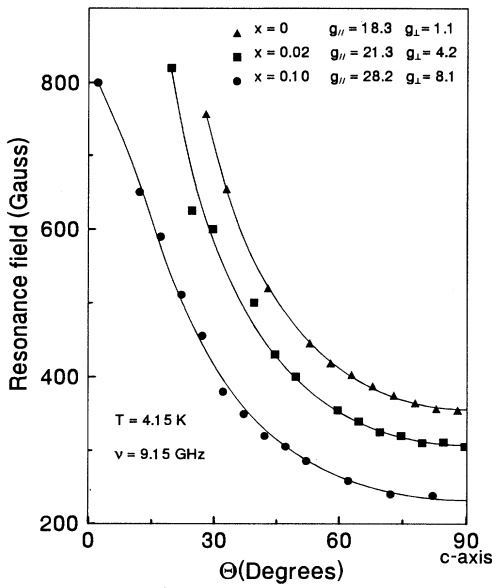

FIG. 8. Angular dependence of the ESR spectra in the (010) plane for Er^{3+} in $Pr_{2-x}Ce_xCuO_4$ ($x = 0$, 0.02, 0.05). Solid lines are the best fit of the resonance field for axial symmetry: $g^2(\theta) = g_{\parallel}^2 \cos^2\theta + g_{\perp}^2 \sin^2\theta$.

to the c axis. It is clear from these data that the effect of inhomogeneities is much stronger than for Gd^{3+}. This is expected since CF effects are first order in non-S-states. Figure 8 shows the anisotropy of the Er^{3+} resonance, which is consistent with the point symmetry at the R site.

IV. CONCLUSIONS

Our ESR data on Gd^{3+} and Er^{3+} in $Pr_{2-x}Ce_xCuO_4$ show that doping with Ce^{4+} produces a rather strong local crystal-field perturbation at the lanthanide site. Our most important finding is a reduction of about 23% in the second-order crystal-field parameter $|b_{20}|$. This may be attributed to charge transfer in the substitution of Ce^{4+} for Pr^{3+} ions. The Ce atoms may act as donor impurities giving electrons to the CuO_2 layers, which in turn modify the CEF at the R site.

It is interesting to note that in INS experiments, Boothroyd *et al.*[6] have observed broader peaks for the Ce doped samples. However the peak at 18 meV shows multiple structure with a main feature at 14 meV. Moreover, Sanjurjo *et al.*[19] also observed recently multiple peak structures in the low-energy part of the Raman CF excitation spectra, similar to that found in the INS experiments. In both experiments, the lower energy peak (14 meV) suggests a reduced $|B_0^2|$ CF parameter for Pr^{3+} in $Pr_{2-x}Ce_x$ CuO_4. The absolute value for a second-order CF parameter weighted among the different sites shown in Table II, $\langle B_0^2 \rangle = \sum_i n_i B_{0i}^2$, gives $|\langle B_0^2 \rangle| \cong$ 24–25 meV. This value is about 21% smaller than the value for Pr_2CuO_4, in good agreement with the ESR result of the present work. The exchange parameter between Gd^{3+} and Pr^{3+} is found to be much smaller than that between Pr^{3+} and Pr^{3+} (see Table II). This is probably due to the larger ionic radius of Pr^{3+} ions. We should mention that in recent INS dispersion experiments in Pr_2CuO_4, Sumarlin *et al.*[24] also interpreted their results in terms of Pr-Pr exchange interaction. As a conclusion, our ESR results suggest that upon doping with Ce there is a charge transfer that modifies the CEF at the lanthanide site.

ACKNOWLEDGMENTS

This work was supported by Grant No. 91/0573-0 of FAPESP, São Paulo-SP-Brazil, and No. NSF-DMR-9117212.

[1] Y. Tokura, H. Takagi, and S. Uchida, Nature (London) **337**, 345 (1989).
[2] H. Takagi, S. Uchida, and Y. Tokura, Phys. Rev. Lett. **62**, 1197 (1989).
[3] J.G. Bednorz and K. Müller, Z. Phys. B **64**, 189 (1986).
[4] A. Wattiaux, J.C. Park, J.C. Grenier, and M. Pouchard, C.R. Acad. Sci. (Paris) **310**, 1047 (1990).
[5] F.C. Chou, D.C. Johnston, S.W. Cheong, and P.C. Canfield, Phys. C **216**, 66 (1993).
[6] A.T. Boothroyd, S.M. Doyle, D. McK. Paul, and R. Osborn, Phys. Rev. B **45**, 10 075 (1992).
[7] M.F. Hundley, J.D. Thompson, S.W. Cheong, Z. Fisk, and S.B. Oseroff, Physica C **158**, 102 (1989).
[8] J.A. Sanjurjo, C. Rettori, S. Oseroff, and Z. Fisk, Phys. Rev. B **49**, 4391 (1994).
[9] C. Rettori, D. Rao, S. Oseroff, R.D. Zysler, M. Tovar, Z. Fisk, S.W. Cheong, S. Schultz, and D.C. Vier, Phys. Rev. B **44**, 826 (1991).
[10] H. Nishihara, H. Yasuoka, T. Shimizu, T. Tsuda, T. Imai, S. Sasaki, S. Kanbe, K. Kishio, K. Kitazawa, and K. Fueki, J. Phys. Soc. Jpn. **56**, 4556 (1987).
[11] K.A. Kubat-Martin, Z. Fisk, and R. Ryan, Acta Crystallogr. C **44**, 1518 (1988).
[12] A. Abragam and B. Bleaney, *EPR of Transition Ions* (Clarendon Press, Oxford, 1970).
[13] J.F. Dyson, Phys. Rev. **98**, 349 (1955); G. Feher and A.F. Kip, *ibid.* **98**, 337 (1955).
[14] W. Low, Phys. Rev. **109**, 265 (1958).
[15] J.M. Tarascon, E. Wang, L.H. Greene, B.G. Bagley, G.W. Hull, S.M. D'Egidio, P.F. Miceli, Z.Z. Wang, T.W. Jing, J. Clayhold, D. Brawner, and N.P. Ong, Phys. Rev. B **40**, 4494 (1989).
[16] D. Davidov, C. Rettori, and D. Shaltiel, Phys. Lett. **50A**, 392 (1974); S. Barners, K. Baberschke, and M. Hardiman, Phys. Rev. B **18**, 2409 (1978), and references therein.
[17] C. Rettori, D. Davidov, A. Grayevsky, and W.M. Walsh, Phys. Rev. B **11**, 4450 (1975).
[18] W.T. Carnall, G.L. Goodman, K. Rajnak, and S. Rana, J. Chem. Phys. **90**, 3443 (1989).
[19] J.A. Sanjurjo, G.B. Martins, P.G. Pagliuso, E. Granado, I. Torriani, C. Rettori, S. Oseroff, and Z. Fisk, Phys. Rev. B **51**, 1185 (1995).
[20] R.D. Zysler, M. Tovar, C. Rettori, D. Rao, H. Shore, S.B. Oseroff, D.C. Vier, S. Schultz, Z. Fisk, and S.W. Cheong, Phys. Rev. B **44**, 9467 (1991).
[21] C. Rettori, D. Rao, S.B. Oseroff, G. Amoretti, Z. Fisk, S.W. Cheong, D.C. Vier, S. Schultz, M. Tovar, and R.D. Zysler, Phys. Rev. B **47**, 8156 (1993).
[22] J.W. Lynn, I.W. Sumarlin, S. Skanthakumar, W-H. Li, R.N. Shelton, J.L. Peng, Z. Fisk, and S.W. Cheong, Phys. Rev. B **41**, 2569 (1990).
[23] I.W. Sumarlin, S. Skanthakumar, J.W. Lynn, J. L. Peng, Z.Y. Li, W. Jiang, and R.L. Greene, Phys. Rev. Lett. **68**, 2228 (1992).
[24] I.W. Sumarlin, J.W. Lynn, T. Chattopadkyay, S.N. Barilo, and D.I. Zhigunov, Physica C **219**, 195 (1994).
[25] In Ref. 9 the value of b_{44} for Pr_2CuO_4 is about five times bigger than that shown in Table I. This is because a wrong Stevens' operator coefficient was used in Ref. 9.